Preliminary Examination

Multi-Sensor Information Acquisition and Fusion

Name: Shuimei Zhang

TUID: 915410782

Department: Electrical & Computer Engineering

Email: shuimei.zhang@temple.edu

Advisor: Dr. Yimin D. Zhang

Contents

1. Introduction

Multisensor data fusion can combine information from various knowledge sources and sensors to provide a better understanding of the phenomenon under consideration [1-2]. Generally, compared with a single sensor, multi-sensor data fusion enjoy many benefits such as improved system reliability and robustness, extended coverage and improved resolution [1]. Here, we are considering multisensor data fusion in a framework of unmanned aerial vehicles (UAVs), due to the increasing importance of UAV these days.

UAVs also known as drones, play a critical role in various civil, military, and homeland security applications, such as disaster monitoring, border surveillance, and relay communications [3-6]. Among these applications, target tracking using UAV is gaining more and more attention, due to its capability of autonomy, especially when there may exist various sources of "threat", obstacles, and restricted areas [7]. UAV target tracking is different with the generic tracking, since UAV aims to locate the target from a low-altitude aerial perspective.

To execute missions that are time critical or span a large geographical area, a single UAV is insufficient due to its limited energy and payload. In addition to the extended coverage, a multi-UAV network also provides diversity gain by sensing an area of interest from different aspect angles to increase the reliability of the estimated target parameters. However, the transmission and fusion of the high volume data between different UAVs pose great challenges as the UAVs are equipped with restricted on-board processing capabilities and have limited communication coverage and data transmission capacities.

Most of the work [6-8] focus on vision-based tracking using UAVs, i.e., using a camera mounted on UAV. In this report, we aim to work on the tracking of multi-targets in a UAV network using passive radar and explore three different but correlated aspects in connection to this area.

2. Robust Adaptive Beamforming

2.1. Beamforming Principle

Beamforming is an effective spatial filtering technique that adjusts the beamforming weight vector to enhance reception of the desired signal and possibly mitigate interference from any other directions. Compared to conventional data-independent beamformers, data dependent beamformers take the array received data into account, and hence are expected to provide better capability for interference suppression.

Consider a narrowband array consisting of M sensors. The array observed signal at time k can be expressed as

$$\begin{aligned} x(k) &= s(k) + i(k) + n(k) \\ &= s(k)a + i(k) + n(k), \end{aligned} \tag{1}$$

where $s(k), i(k)$ and $n(k)$ are the desired signal, interference and noise respectively. The desired signal can be written as $x(k) = s(k)a$, where $s(k)$ is the signal waveform and $a \in \mathbb{C}^M$ is the associated steering vector.

The senor output is weighted by $w_m^*, m = 1, \cdots, M$, then the output of adaptive beamformer is given by

$$y(k) = \sum_{m=1}^{M} w_m^* x_m(k) = \begin{bmatrix} w_1^* & w_2^* & \cdots & w_M^* \end{bmatrix} x(k) = w^H x(k). \tag{2}$$

2.2. Model Mismatch

The optimal beamforming weight vector w can be obtained by maximizing the output signal-to-noise ratio (SINR)

$$\text{SINR}(w) = \frac{E\left\{\left| w^H a s(k) \right|^2\right\}}{E\left\{\left| w^H \left[i(k) + n(k) \right] \right|^2\right\}} = \frac{\sigma_s^2 \left| w^H a \right|^2}{w^H R_{i+n} w}, \tag{3}$$

where $E\{\bullet\}$ is the statistical expectation, σ_s^2 is the signal power and $R_{i+n} \in \mathbb{C}^{M \times M}$ is the interference-plus-noise covariance matrix. The optimal beamforming weight vector can be

obtained by maximizing the output SINR which is equivalent to the minimum variance distortionless response (MVDR) beamformer (also referred to Capon beamformer) beamforming problem

$$\min_{w} \quad w^H R_{i+n} w$$
$$\text{subject to} \quad w^H a = 1. \tag{4}$$

Using Lagrange multiplier method, we can easily obtain the solution as

$$w_{\text{opt}} = \frac{R_{i+n}^{-1} a}{a^H R_{i+n}^{-1} a}. \tag{5}$$

We can notice that the optimal beamforming weight is a function of R_{i+n} and a.

In practice, R_{i+n} is unavailable and it is usually replaced by the sample covariance matrix

$$R = \frac{1}{K} \sum_{k=1}^{K} x(k) x^H(k). \tag{6}$$

Also, the steering vector a may be inaccurate due to imperfect calibration, look direction error and scattering effects. Therefore, it is necessary to propose a robust adaptive beamforming method to address the model mismatch issue.

2.3. Reconstruction-Plus-Estimation-Based Adaptive Beamforming Algorithm

In the paper [10], the author proposed a two-stage strategy to deal with the model mismatch issue. In the first stage, the interference-plus-noise covariance matrix is reconstructed. In the second stage, the actual steering vector is estimated.

2.3.1. Interference-Plus-Noise Covariance Matrix Reconstruction

To reconstruct the interference-plus-noise covariance matrix, the spatial spectrum distribution over all possible directions are required to be known. The interference-plus-noise covariance matrix R_{i+n} can be reconstructed as

$$\hat{R}_{i+n} = \int_{\bar{\Theta}} \hat{p}_{\text{Capon}}(\theta) a^H(\theta) a(\theta), \tag{7}$$

where $a(\theta)$ is the steering vector associated with a hypothetical direction θ,

3

$$\hat{p}_{\text{Capon}} = \frac{1}{a^H(\theta)\hat{R}^{-1}a(\theta)}, \tag{8}$$

is the Capon spatial spectrum estimator and $\bar{\Theta}$ is the complement sector of Θ. Here, Θ is a known or estimated angular sector where the desired signal is located. In other words, $\bar{\Theta}$ effectively excludes the desired signal.

2.3.2. Desired Signal Steering Vector Estimation

In this subsection, the presumed steering vector is corrected via the maximization of the beamformer output power. Here, the presumed steering vector means that steering vector associated with the nominal DOA on the known array structure.

Since the reconstructed interference-plus-noise covariance matrix $\hat{R}_{i+n}$ is obtained in the first stage, the beamformer output power can be expressed as

$$p(a) = \frac{1}{a^H \hat{R}_{i+n}^{-1} a}. \tag{9}$$

Maximizing the beamformer output power is equivalent to minimize the denominator of $p(a)$. To exclude trivial solution $a = 0$, the presumed steering vector $\bar{a}$ is utilized. Given $a = \bar{a} + e$, the optimization problem can be transformed as

$$\begin{aligned} \min_{e} \quad & (\bar{a} + e)^H \hat{R}_{i+n}^{-1} (\bar{a} + e) \\ \text{subject to} \quad & (\bar{a} + e)^H \hat{R}_{i+n} (\bar{a} + e) \le \bar{a}^H \hat{R}_{i+n} \bar{a}, \end{aligned} \tag{10}$$

where the constraint is used to prevent the corrected steering vector $a = \bar{a} + e$ from converging to any interference located in $\bar{\Theta}$.

The mismatch vector can be further decomposed into two components, $e_{\perp}$ which is orthogonal to $\bar{a}$, and $e_{\parallel}$ which is parallel to $\bar{a}$. $e_{\parallel}$ will not affect the beamforming quality, since it is a scaled copy of $\bar{a}$. Then the optimization problem is simplified to find the orthogonal component $e_{\perp}$, which is expressed as

4

$$\min_{e_\perp} \qquad \left(\bar{a}+e_\perp\right)^H \hat{R}_{i+n}^{-1}\left(\bar{a}+e_\perp\right)$$

$$\text{subject to} \qquad \bar{a}^H e_\perp = 0, \tag{11}$$

$$\left(\bar{a}+e_\perp\right)^H \hat{R}_{i+n}\left(\bar{a}+e_\perp\right) \le \bar{a}^H \hat{R}_{i+n}\bar{a}.$$

The problem is a feasible quadratically constrained quadratic programming (QCQP) problem and can be easily solved using CVX.

By now, the actual steering vector is estimated as

$$\tilde{a} = \bar{a}+e_\perp, \tag{12}$$

and the optimal beamforming weight vector is

$$w_{\text{Rec-Est}} = \frac{\hat{R}_{i+n}^{-1}\tilde{a}}{\tilde{a}^H \hat{R}_{i+n}^{-1}\tilde{a}}. \tag{13}$$

2.4. Simulation Results

Consider a 10-element uniform linear array with spaced half wavelength apart. The zero mean spatially white Gaussian noise is considered. Two interfering sources are assumed to have DOAs $-50°$ and $-20°$, respectively. The interference-to-noise ratio (INR) in each sensor is equal to 30 dB. The desired signal is assumed to be a plane-wave from the presumed direction $\theta_s = 5°$. If not specified, the number of snapshots is 30 and the SNR in each sensor is set to be fixed at 20 dB. 200 Monte-Carlo runs are performed for each scenario.

Here, the scenario of random signal and interference look direction mismatch is considered. A uniform distributed mismatch with a range $\left[-4°, 4°\right]$ is added to all the interference and signal directions for each run (not snapshot). From Figure 1, we know that the proposed beamformers are always close to the optimal SINR from -30 to 50 dB and enjoy much faster convergence rates than others.
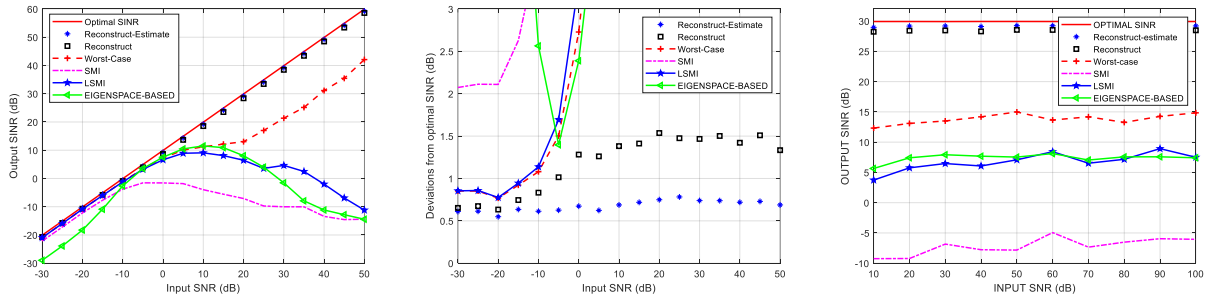
(a)Output SINR versus input SNR (b) Deviations from optimal SINR versus SNR (c) Output SINR versus number of snapshots

Figure 1 The results for random signal and interference look direction mismatch

2.5. Comments in the Context of Multi-Sensor Information Fusion

Robust adaptive beamforming is important for the multi-target tracking using a UAV network. It is common that signal reflecting from targets are affected by the local scatter effects. Also, if the antenna array are not perfectly calibrated, it is difficult to obtain the actual locations of the targets. What is more, UAV tends to have sudden movements. Robust adaptive beamforming can mitigate the effects of model mismatch while suppress the interference.

6

3. Sparsity-Based Signal Processing

3.1. Basis Mismatch

Compressed sensing indicates that the required number of samples for reconstructing a signal can be greatly reduced if it is sparse in a known discrete basis. However, many real-world signals are sparse in a continuous dictionary. In the presence of basis mismatch, exact or near-exact sparse recovery cannot be guaranteed. Recovery may suffer large errors.

The paper [15] developed for parameter estimation without discretization with theoretical guarantees. The atomic nom minimization based method is developed to deal with off-grid issue.

3.2. Atomic Norm of the MMV Model

In a multiple measurement vectors (MMV) model, we consider L spectrally-sparse signal with r distinct frequency components, stacked in a matrix as

$$X = [x_1, \ldots, x_L], \ l = 1, \cdots, L, \tag{14}$$

where each signal is

$$x_l = \sum_{k=1}^{r} c_{k,l} a(f_k) = Vc_l \in \mathbb{C}^n, \tag{15}$$

with $\quad c_l = [c_{1,l}, \ldots, c_{r,l}]^T \in \mathbb{C}^r \quad, \quad a(f) = \frac{1}{\sqrt{n}} [1, e^{j2\pi f}, \ldots, e^{j2\pi f(n-1)}]^T, \ f \in [0,1) \quad$ and

$V = [a(f_1), \ldots, a(f_r)] \in \mathbb{C}^{n \times r}$. Here, the set of frequencies can lie anywhere on the unit interval, so that f_k is continuous-valued $[0,1)$. X can be further expressed as

$$X = VC \in \mathbb{C}^{n \times L} \tag{16}$$

where $C = [c_1, \ldots, c_L] \in \mathbb{C}^{r \times L}$.

The concept of atomic norm was first proposed in [11] and was proposed to find tightest convex relaxations of general parsimonious models including sparse signals as a special case. Generally, we have three steps to achieve the minimization of atomic norm.

Step 1: Define an atom for representing X as

$$A(f, b) = a(f) b^* \text{ where } f \in [0,1), b \in \mathbb{C}^L \text{ with } \|b\|_2 = 1. \tag{17}$$

The atomic set is $\mathcal{A} = \left\{ A(f, b) \mid f \in [0,1), \|b\|_2 = 1 \right\}$.

Step 2: Define the atomic norm of X as

$$\| X \|_{\mathcal{A}} = \inf\{ t > 0 : X \in t \operatorname{conv}(\mathcal{A}) \} = \inf \left\{ \sum_k c_k \mid X = \sum_k c_k A(f_k, b_k), c_k \geq 0 \right\}, \tag{18}$$

where $\operatorname{conv}(\mathcal{A})$ is the convex hull of $\mathcal{A}$.

Step 3: Formulate a convex program to minimize the atomic norm.

$$\| X \|_{\mathcal{A}} = \inf_{u \in \mathbb{C}^n, W \in \mathbb{C}^{L \times L}} \left\{ \frac{1}{2} \operatorname{Tr}(\mathcal{T}(u)) + \frac{1}{2} \operatorname{Tr}(W) \left| \begin{bmatrix} \mathcal{T}(u) & X \\ X^* & W \end{bmatrix} \succeq 0 \right. \right\}. \tag{19}$$

3.3. Signal Recovery with Atomic Norm

In the absence of noise, we follow the atomic norm minimization algorithm to recover the complete signal $X^\star$

$$X = \arg \min_X \| X \|_{\mathcal{A}} \quad \text{s.t.} \quad X_{\bar{\Omega}} = Z_{\bar{\Omega}}, \tag{20}$$

where $\bar{\Omega} \subset \{0, \ldots, n-1\} \times \{1, \ldots, L\}$ denotes the observation pattern. Then the signal recovery problem can be solved via

$$\begin{aligned} X = \arg \min_X \inf_{u, W} \quad & \frac{1}{2} \operatorname{Tr}(\mathcal{T}(u)) + \frac{1}{2} \operatorname{Tr}(W) \\ \text{s.t.} \quad & \begin{bmatrix} \mathcal{T}(u) & X \\ X^* & W \end{bmatrix} \succeq 0, X_{\bar{\Omega}} = Z_{\bar{\Omega}}. \end{aligned} \tag{21}$$

Assume the phase of the coefficients are drawn i.i.d. from the uniform distribution on the complex unit circle and the minimum separation between frequency pairs wrapped on the unit circle meets the following requirement

$$\Delta := \min_{k \neq l} |f_k - f_l| \geq \frac{1}{\lfloor (n-1)/4 \rfloor}. \tag{22}$$

Then there exists a numerical constant C such that

$$|\bar{\Omega}| \geq CL \max\left\{\log^2 \frac{n}{\delta}, r\log\frac{r}{\delta}\log\frac{n}{\delta}\right\}, \tag{23}$$

is sufficient to guarantee exact recovery with probability at least $1 - L\delta$.

For the single vector, it is possible to employ the atomic norm minimization for the MMV model. Construct a Hankel matrix from $x = \sum_{k=1}^{r} c_k a(f_k)$, the Hankel matrix with a pencil parameter p is as follows

$$\mathcal{H}(x, p) = \begin{bmatrix} x_1 & x_2 & \cdots & x_{n-p+1} \\ x_2 & x_3 & \cdots & x_{n-p+2} \\ \vdots & \vdots & \ddots & \vdots \\ x_p & x_{p+1} & \cdots & x_n \end{bmatrix}. \tag{24}$$

The columns can be viewed as an ensemble of spectrally-sparse signals sharing the same frequencies. Recover x by minimizing the atomic norm of $\mathcal{H}(x, p)$,

$$\hat{x}_A = \arg\min_x \|\mathcal{H}(x, p)\|_A \quad \text{s.t. } x_\Omega = z_\Omega, \tag{25}$$

which can be reformulated as

$$\min_{u, W_2, x} \mathrm{Tr}(\mathcal{T}(u)) + \mathrm{Tr}(W_2)$$
$$\text{s.t. } \begin{bmatrix} \mathcal{T}(u) & \mathcal{H}(x, p) \\ \mathcal{H}(x, p)^* & W_2 \end{bmatrix} \succeq 0, x_\Omega = z_\Omega. \tag{26}$$

3.4. Structured Covariance Estimation

In many applications, people only interested in frequencies, and the covariance matrix of the signal carries sufficient information to recover the frequencies. Given that the coefficients from different signals are uncorrelated, and the coefficients for different frequencies in the same signal are also uncorrelated.

$$\mathbb{E}\left[c_{k,l}c_{k',l'}\right] = \begin{cases} \sigma_k^2, & \text{if } k = k', l = l' \\ 0, & \text{otherwise} \end{cases}. \tag{27}$$

The covariance matrix of signal x_l can be written as

$$\boldsymbol{\Sigma}^{\star} = \mathbb{E}\left[\boldsymbol{x}_l \boldsymbol{x}_l^*\right] = \sum_{k=1}^{r} \sigma_k^2 \boldsymbol{a}\left(f_k\right) \boldsymbol{a}\left(f_k\right)^* = \mathcal{T}\left(\boldsymbol{u}^{\star}\right) \in \mathbb{C}^{n \times n}, \tag{28}$$

where $\boldsymbol{u}^{\star} = \dfrac{1}{\sqrt{n}} \sum_{k=1}^{r} \sigma_k^2 \boldsymbol{a}\left(f_k\right) \in \mathbb{C}^n$ is the first column of $\boldsymbol{\Sigma}^{\star}$. From $\boldsymbol{u}^{\star}$ or $\boldsymbol{\Sigma}^{\star}$, the set of frequencies

can be estimated by spectrum estimation algorithms such as MUSIC [12] and ESPRIT [13].

The covariance matrix of the partially observed samples $\boldsymbol{x}_{\Omega,l}$ can be given as

$$\boldsymbol{\Sigma}_{\Omega}^{\star} = \mathbb{E}\left[\boldsymbol{x}_{\Omega,l} \boldsymbol{x}_{\Omega,l}^*\right] = \mathcal{P}_{\Omega}\left(\boldsymbol{\Sigma}^{\star}\right) \in \mathbb{C}^{m \times m}. \tag{29}$$

The ideal covariance matrix is unavailable and is approximated by

$$\boldsymbol{\Sigma}_{\Omega,L} = \frac{1}{L} \sum_{l=1}^{L} \boldsymbol{x}_{\Omega,l} \boldsymbol{x}_{\Omega,l}^* = \frac{1}{L} \boldsymbol{X}_{\Omega} \boldsymbol{X}_{\Omega}^* \in \mathbb{C}^{m \times m}. \tag{30}$$

The problem of covariance matrix estimation is formulated to seek a low-rank PSD Hermitian Toeplitz matrix whose entries indexed by Ω is close to the sample covariance matrix $\boldsymbol{\Sigma}_{\Omega,L}$. The frequency estimation problem from partial observation can be

$$\boldsymbol{u} = \arg \min_{\boldsymbol{u} \in \mathbb{C}^n} \frac{1}{2} \left\| \mathcal{P}_{\Omega}(\mathcal{T}(\boldsymbol{u})) - \boldsymbol{\Sigma}_{\Omega,L} \right\|_F^2 + \lambda \operatorname{rank}(\mathcal{T}(\boldsymbol{u})) \atop \text{s.t. } \mathcal{T}(\boldsymbol{u}) \succeq 0, \tag{31}$$

where is a regularization parameter balancing the data fitting term and the rank regularization term. However, this problem is not convex, which can be relaxed as

$$\boldsymbol{u} = \arg \min_{\boldsymbol{u} \in \mathbb{C}^n} \frac{1}{2} \left\| \mathcal{P}_{\Omega}(\mathcal{T}(\boldsymbol{u})) - \boldsymbol{\Sigma}_{\Omega,L} \right\|_F^2 + \lambda \operatorname{Tr}(\mathcal{T}(\mathbf{u})) \atop \text{s.t. } \mathcal{T}(\boldsymbol{u}) \succeq 0. \tag{32}$$

Given that $\|\boldsymbol{u}\|_{\mathcal{A}} = \operatorname{Tr}(\mathcal{T}(\boldsymbol{u}))$, if $\mathcal{T}(\boldsymbol{u}) \succeq 0$, the optimization problem is actually an atomic norm regularized algorithm

$$\boldsymbol{u} = \arg \min_{\boldsymbol{u} \in \mathbb{C}^n} \frac{1}{2} \left\| \mathcal{P}_{\Omega}(\mathcal{T}(\boldsymbol{u})) - \boldsymbol{\Sigma}_{\Omega,L} \right\|_F^2 + \lambda \|\boldsymbol{u}\|_{\mathcal{A}} \atop \text{s.t. } \mathcal{T}(\boldsymbol{u}) \succeq 0. \tag{33}$$

3.5. Simulation Results

Here, we compare qualitatively the performance of frequency estimation using different algorithms, including CS using group sparsity with a DFT frame [14], atomic norm minimization, and structured covariance estimation. Consider $n = 64$, $r=6$, $L=400$. Only 8 elements are observed. For CS using group sparsity with a DFT frame, the dictionary size is 64×256. We can notice that for CS with DFT frame, due to the off-grid mismatch, CS predicts frequencies on the lattice of the DFT frame, and results in a larger number of estimated frequencies. For atomic norm minimization, it fails to distinguish the two close frequencies and misses one frequency due to insufficient number of measurements per vector. For structured covariance estimation, it works well to locate all the frequencies.

(a) Ground truth

(b) CS with DFT frame

(c) Atomic norm minimization

(d) Structured covariance estimation
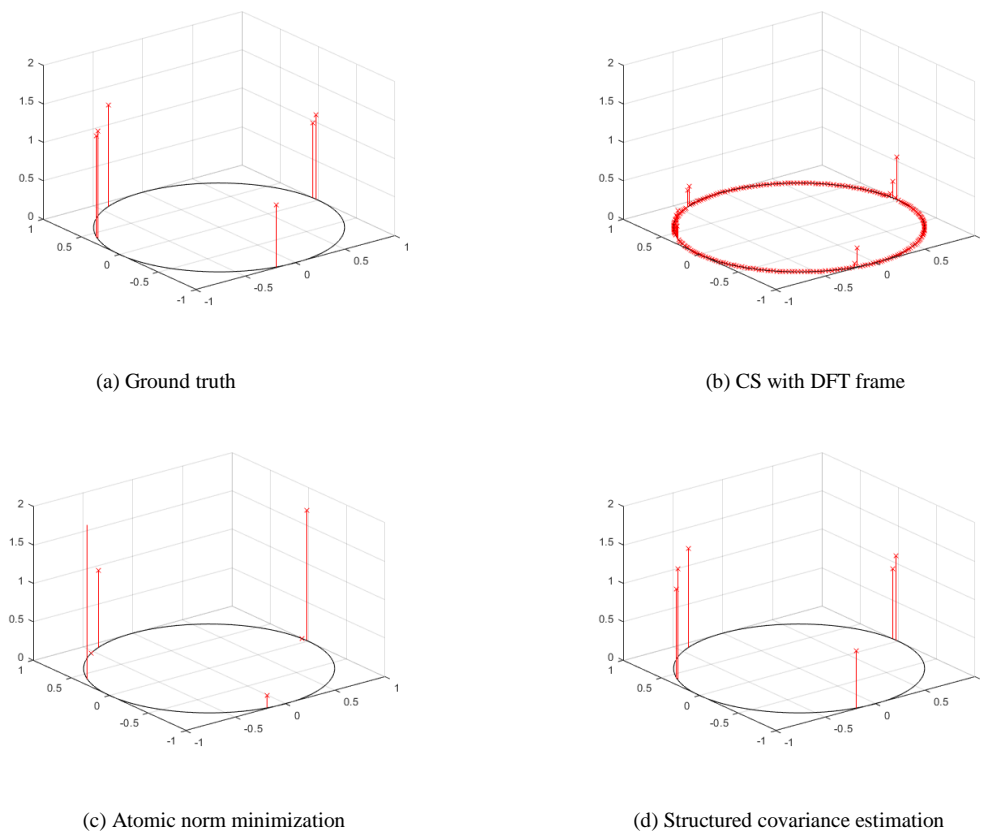
Figure 2 Frequency estimation with noiseless measurements using different algorithms when n=64, L=400, m=8 and r = 6.

3.6. Comments in the Context of Multi-Sensor Information Fusion

Compressive sensing can be used to solve sparse reconstruction problems in order to provide high-quality signal reconstruction. The target state search space, representing the position and velocity of the targets, is sparsely populated because the targets are sparsely distributed within the surveillance area. This fact enables sparsity-based approaches to be applied in the conventional distributed stationary radars. However, for compressive sensing, it is sensitive to basis mismatch. This paper provides a procedure to address this issue and is necessary to be well studied.

4. Multi-Target Tracking

4.1. Signal Model

Multi-target tracking (MTT) refers to a problem of jointly estimating the number of targets and their states (positions, velocity, etc.), at successive time intervals, from a noisy and cluttered set of observations. For Doppler-only tracking, it offers two key advantages. One is that strictly synchronous operation among the sensors is not required. The other one is that the required volume of information exchange is significantly reduced.

In this paper [16], the author utilizes a multi-static passive radar (MPR) system to track multiple time varying ground moving targets. One broadcast station with carrier frequency f_c, located at b. N spatially distributed Doppler sensors, located at $\mathbf{r}^{(n)}, n = 1, \ldots, N$. The transmitter and the Doppler sensors are assumed stationary and their locations are assumed to be known.

The state vector of the ith target at time k, $\mathbf{X}_{k,i}$, is a point in the state space $\mathbb{X} \in \mathbb{R}^{4 \times 1}$ and can be written as

$$\mathbf{x}_{k,i} = \left[\mathbf{p}_{k,i}^T, \mathbf{v}_i^T \right]^T, \tag{34}$$

where $\mathbf{p}_{k,i} \triangleq \left[p_{x,k,i}, p_{y,k,i} \right]^T$ and $\mathbf{v}_i \triangleq \left[v_{x,i}, v_{y,i} \right]^T$. The target dynamics is modeled as a linear Gaussian nearly constant velocity model as

$$\mathbf{x}_{k,i} = \mathbf{F}\mathbf{x}_{k-1,i} + \mathbf{G}\mathbf{w}_{k,i}, i = 1, \ldots, T(k), \tag{35}$$

where $T(k)$ denotes the number of targets at the at the kth observation and the state transition matrix is defined as

$$\mathbf{F} = \begin{bmatrix} \mathbf{I}_2 & \Delta\mathbf{I}_2 \\ \mathbf{0}_2 & \mathbf{I}_2 \end{bmatrix}. \tag{36}$$

The transitions matrix

$$\mathbf{G} = \begin{bmatrix} \dfrac{\Delta^2}{2}\mathbf{I}_2 \\ \Delta\mathbf{I}_2 \end{bmatrix}, \tag{37}$$

accounts for the small acceleration that could deviate the target trajectory from being strictly linear. The actual bistatic Doppler frequency at the nth sensor due to the motion of the ith target is obtained as

$$\hat{f}_{k,i}^{(n)} = -\frac{\mathbf{v}_i^T}{\lambda}\left[\frac{\mathbf{p}_{k,i} - \mathbf{r}^{(n)}}{\left\|\mathbf{p}_{k,i} - \mathbf{r}^{(n)}\right\|} + \frac{\mathbf{p}_{k,i} - \mathbf{b}}{\left\|\mathbf{p}_{k,i} - \mathbf{b}\right\|}\right], \tag{38}$$

where $\lambda = c/f_c$ is the wavelength.

In practice, the Doppler frequency measurements are subject to additive noise, missed detection and measurement uncertainties. The measured Doppler frequencies are

$$f_{k,i}^{(n)} = \begin{cases} \breve{f}_{k,i}^{(n)} + \epsilon_{k,i}^{(n)}, & \text{if } \rho_{k,i}^{(n)} = 1 \\ \varnothing, & \text{if } \rho_{k,i}^{(n)} = 0 \end{cases}, \tag{39}$$

where $\rho_{k,i}^{(n)} \in \{0,1\}$ is a Bernoulli random variable and $\epsilon_{k,i}^{(n)} \sim \mathcal{N}\left(0, \sigma_\epsilon^2\right)$. The actual target generated measurements at the kth observation can de expressed as

$$\mathcal{T}_k^{(n)} = \left\{f_{k,1}^{(n)}, \ldots, f_{k,\tau(k)}^{(n)}\right\}, \quad \tau(k) \le T(k). \tag{40}$$

Incorporating the effects of clutter, the observed Doppler measurements are

$$\mathcal{D}_k^{(n)} = \mathcal{T}_k^{(n)} \bigcup \mathcal{K}_k^{(n)}. \tag{41}$$

where $\mathcal{K}_k^{(n)}$ denotes the clutter.

4.2. Multi-Senor Measurement Fusion Exploiting Group Sparsity

The entire Doppler spectrum corresponding to $\mathcal{D}_k^{(n)}$ can be expressed as

$$Y_k^{(n)}(f) = \sum_{i=1}^{D(k)} \delta\left(f - f_{k,i}^{(n)}\right), \tag{42}$$

and the 'pseudo-measurement' in the time-domain as

$$y_k^{(n)}(t) = \sum_{i=1}^{D(k)} \exp\left(j2\pi f_{k,i}^{(n)} t + \phi_0\right). \tag{43}$$

14

Without loss of generality, ϕ_0 is set to 0. Given that the measure Doppler frequency may not be accurate, we have

$$
\begin{aligned}
y_k^{(n)}(t) &= \sum_{i=1}^{D(k)} \exp\left(j2\pi f_{k,i}^{(n)} t \right) \\
&= \sum_{i=1}^{D(k)} \exp\left(j2\pi \left(\breve{f}_{k,i}^{(n)} + \epsilon_{k,i}^{(n)} \right) t \right) \\
&= \sum_{i=1}^{D(k)} \exp\left(j2\pi \breve{f}_{k,i}^{(n)} t \right) \exp\left(j2\pi \epsilon_{k,i}^{(n)} t \right).
\end{aligned}
\tag{44}
$$

Utilizing Taylor series expansion

$$
\exp\left(j2\pi \epsilon_{k,i}^{(n)} \right) = 1 + \sum_{q=1}^{\infty} \frac{\left(j2\pi \epsilon_{k,i}^{(n)} t \right)^q}{q!} \triangleq 1 + \zeta(t),
\tag{45}
$$

where q is the order of expansion, we have

$$
y_k^{(n)}(t) = \sum_{i=1}^{D(k)} \exp\left(j2\pi \tilde{f}_{k,i}^{(n)} t \right) + \xi_{k,i}^{(n)}(t), \ \ \xi_{k,i}^{(n)}(t) = \zeta(t) \exp\left(j2\pi \breve{f}_{k,i}^{(n)} t \right).
\tag{46}
$$

The entire target state space is represented by a 4-D discrete space comprising $M = M_{px} M_{py} M_{vx} M_{vy}$ points, and each point representing a possible target state vector. The corresponding Doppler frequency measurement at sensor n can be obtained as

$$
\tilde{f}_{k,\tau}^{(n)} = -\frac{\mathbf{v}_\tau^T}{\lambda} \left[\frac{\tilde{\mathbf{p}}_{k,\tau} - \mathbf{r}^{(n)}}{\left\| \tilde{\mathbf{p}}_{k,\tau} - \mathbf{r}^{(n)} \right\|} + \frac{\tilde{\mathbf{p}}_{k,\tau} - \mathbf{b}}{\left\| \tilde{\mathbf{p}}_{k,\tau} - \mathbf{b} \right\|} \right],
\tag{47}
$$

and the corresponding hypothetical 'pseudo-measurement' vector is

$$
\tilde{y}_{k,\tau}^{(n)}(t) = \exp\left(j2\pi \tilde{f}_{k,\tau}^{(n)} t \right), \ t = 1, \ldots, N_s.
\tag{48}
$$

The multi-static Doppler measurements share a common ground truth in the position-velocity space, the unknown sparse vectors representing the target state space $\mathbf{u}_k^{(n)}$ can be obtained as the group sparse solution. The problem can be formulated as

$$
\mathbf{y}_k^{(n)} = \Psi_k^{(n)} \mathbf{u}_k^{(n)} + \xi_k^{(n)}, \quad n = 1, \ldots, N,
\tag{49}
$$

where $\mathbf{y}_k^{(n)} = \left[y_k^{(n)}(1),\ldots, y_k^{(n)}(N_s) \right]^T \in \mathbb{C}^{N_s \times 1}$ denotes the observed vector and the Dictionary matrix

with the τ th column is $\psi_{k,\tau}^{(n)} = \left[\tilde{y}_{k,\tau}^{(n)}(1),\ldots, \tilde{y}_{k,\tau}^{(n)}(N_s) \right]^T$. The group sparse problem in (49) can be

solved by a lot of algorithms such as block orthogonal matching [17] and multi-task Bayesian compressive sensing (MTCS) [18].

4.3. Random Finite Set Based Filtering

The target state estimates from the group sparse solution may contain the target estimates of the clutter, small number of spurious estimates that may occur occasionally during the group sparse reconstruction due to the additive noise and missed detection. It is necessary to perform a procedure which can filter the false measurements and compensate the missed detection. A random finite set (RFS) is a set of random variables (or vectors) whose cardinality is also a random variable. In a tracking algorithm, a RFS can be used to model the multi-target state, while the random variable associated to the set cardinality allows us to model target presence uncertainty. The key point is that the target set is modelled as the state set, and the measurement set is modelled as the observation set, such that the tracking problem is transformed to a filtering problem with state space and observation space.

A RFS model for the time evolution of a multi-target state $\mathcal{X}_k$ at time k from $\mathcal{X}_{k-1}$ is defined as

$$\mathcal{X}_k = \left[\bigcup_{\zeta \in \mathcal{K}_{k-1}} \mathcal{S}_{k|k-1}(\zeta) \right] \cup \Gamma_k, \tag{50}$$

where $\mathcal{S}_{k|k-1}(\zeta)$ represents the RFS of the surviving targets from the preceding state ζ, and Γ_k is the RFS of the spontaneous target births at k.

The corresponding RFS measurement model observed at the kth observation can be expressed as

$$\mathcal{Z}_k = \Upsilon_k \bigcup \left[\bigcup_{x \in \mathcal{X}_k} \Theta_k(x) \right], \tag{51}$$

where Υ_k represents the RFS of the clutter measurements and the false estimates that occur during the group sparse reconstruction, and $\Theta_k(x)$ is the RFS of the actual target-generated measurements. The multi-target posterior density $p_k(.|Z_{1:k})$ can be determined using the Bayesian recursion

$$p_{k|k-1}(X_k|Z_{1:k-1}) = \int f_{k|k-1}(X_k|X) p_{k-1}(X|Z_{1:k-1}) dX, \tag{52}$$

and

$$p_k(X_k|Z_{1:k}) = \frac{g_k(Z_k|X_k) p_{k|k-1}(X_k|Z_{1:k-1})}{\int g_k(Z_k|X) p_{k|k-1}(X|Z_{1:k-1}) dX}. \tag{53}$$

The probability hypothesis density (PHD) filter is to alleviate the computational intractability in the multiple-target Bayes filter. Instead of propagating the multiple-target posterior density in time, the PHD filter propagates the posterior intensity, a first-order statistical moment of the posterior multiple-target state. The Gaussian mixture PHD (GMPHD) filter propagates the Gaussian mixture posterior intensity.

4.4. Simulation Results

Consider a broadcast station at the origin transmitting at 950 MHz, and 5 Doppler sensors distributed along a circle of radius 2.5 km from the transmitter as shown in Figure 3. The simulation parameters are illustrated in Table 1.
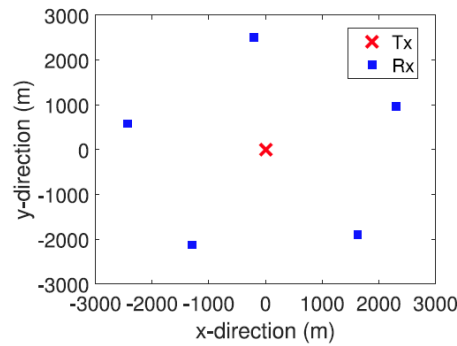
Figure 3 Passive multi-static radar network configuration using multiple Doppler sensors.

Table 1 Simulation Parameters

Parameter	Value
Sampling interval (Δ)	0.5 s
Observation period of the 'pseudo-measurement'(Δy)	1 s
Maximum possible Doppler frequency measurement (f_0)	250 Hz
Sampling rate of the 'pseudo-measurement' (F_s)	512 Hz
Standard deviation of process noise (σ_w)	1 m/s^2
Frequency of operation	950 MHz
Standard deviation of measurement noise (σ_ϵ)	0.3 Hz
Probability of target detection (p_D)	0.98
Probability of target survival (p_S)	0.99

We consider non-crossing target trajectories with linear constant velocity. Two targets are initially located at $[-1000, 0]^T$ m, and $[1000, 0]^T$ m and travelling along linear trajectories with velocities $[30, 30]^T$ m/s and $[-30, -30]^T$ m/s, respectively as shown in Figure 4. MTCS is utilized for the group sparse problem. The algorithm yields the estimated target positions closely grouped around the actual target trajectories throughout the observation period. But we cannot discern between the true target generated measurements and the clutter generated measurements. The tracking filter reduces the overall cardinality and localization errors by removing the false measurements, compensating for the missed detections, and smoothing the true target state estimates.

(a) Ground truth   (b) Instantaneous target state estimation   (c) Result of the GMPHD filter
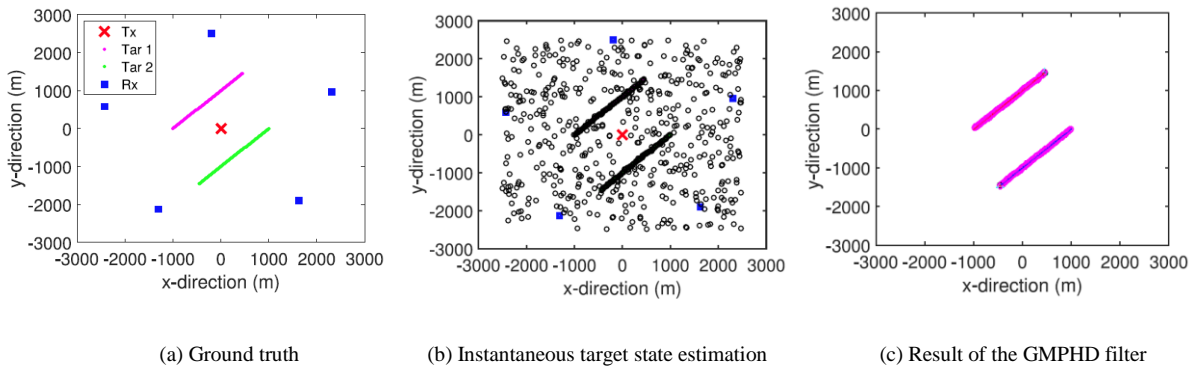
Figure 4 Tracking result using group sparsity and GMPHD filter

4.5. Comments in the Context of Multi-Sensor Information Fusion

This paper provides a framework for my future work. In this paper, estimated Doppler frequency measurements are transmitted to the fusion center instead of the raw data. This can motivates the similar ways to reduce the communication bandwidth, due to the restricted data transmission capacity of the UAV. Also, due to the common sparse support for different receivers, group sparsity can be utilized. This property can be used to improve the tracking performance.

5. Summary

Three research articles are discussed in the report in connection with the future research work of multi-sensor information fusion, especially in the application of multi-target tracking using a UAV network. In the first article, one two-stage robust adaptive beamforming method is proposed to mitigate the model mismatch issue while maintains the capability to suppress the interference. In the second article, off-grid method is discussed, which can be useful when we are doing compressive sensing and the issue of basis mismatch can be addressed. Robust adaptive beamforming can be combined with sparsity-based method to obtain a reliable high-resolution localization result. In the third paper, it provides us a framework to do multi-target tracking using passive radars. Just like this paper, the state estimates can be transmitted between UAVs instead of the raw data, such that the communication bandwidth can be reduced.

Reference

[1]. D. Hall and J. Llinas, "An introduction to multisensor data fusion," *Proc. IEEE*, vol. 85, no. 1, pp. 6 –23, Jan 1997. [Online]. Available: http://dx.doi.org/10.1109/5.554205

[2]. B. Khaleghi, A. Khamis, F. O. Karray, and S. N. Razavi, "Multisensor data fusion: A review of the state-of-the-art," *Inf. Fusion*, vol. 14, no. 1, pp. 28–44, 2013.

[3]. A. Ryan, M. Zennaro, A. Howell, R. Sengupta, and J. Hedrick,"An overview of emerging results in cooperative UAV control," in *Proc. IEEE Conf. Decision and Control*, Nassau, Bahamas, May 2004, pp. 602–607.

[4]. R. C. Palat, A. Annamalai, and J. H. Reed, "Cooperative relay-ing for ad hoc ground networks using swarms," in *Proc. IEEE Milit. Comm. Conf.*, Atlantic City, NJ, Nov. 2005, pp. 1588–1594.

[5]. Li and Y. D. Zhang, "Multi-source cooperative communications using multiple small relay UAVs," in *Proc. IEEE Globe-com Workshop on Wireless Networking for Unmanned Aerial Vehicles*, Miami, FL, Dec. 2010, pp. 1805–1810.

[6]. S. Hayat, E. Yanmaz, and R. Muzaffar, "Survey on unmanned aerial vehicle networks for civil applications: A communications viewpoint," *IEEE Commun. Surveys Tut.,* vol. 18, no. 4,pp. 2624–2661, 2016.

[7]. U. Zengin and A. Dogan, "Real-time target tracking for autonomous UAVs in adversarial environments: A gradient search algorithm," *IEEE Trans. Robot.,* vol. 23, no. 2, pp. 294–307, Apr. 2007.

[8]. M. Mueller, N. Smith, and B. Ghanem, "A benchmark and simulator for UAV tracking," in *Proc. Eur. Conf. Comput. Vis. (ECCV),* 2016, pp. 445–461

[9]. K. Song, W. Zhang, and X. Rong, "UAV target tracking with a boundary decision network," in *Proc. Int. Conf. Pattern Recognit. (ICPR),* 2018, pp. 2576–2581.

[10]. Y. Gu and A. Leshem, "Robust adaptive beamforming based on interference covariance matrix reconstruction and steering vector estimation," *IEEE Trans. Signal Process.,* vol. 60, no. 7, pp. 3881–3885, Jul. 2012.

[11]. V. Chandrasekaran, B. Recht, P. A. Parrilo, A. S. Willsky, The convex geometry of linear inverse problems, *Foundations of Computational Mathematics* 12 (6) (2012) 805–849.

[12]. R. Schmidt, "Multiple emitter location and signal parameter estimation," *IEEE Trans. Antennas Propag.,* vol. AP-34, no. 3, pp. 276–280, Mar. 1986.

[13]. R. Roy and T. Kailath, "ESPRIT-estimation of signal parameters via rotational invariance techniques," *IEEE Trans. Acoust., Speech Signal Process.,* vol. 37, no. 7, pp. 984–995, Jul. 1989.

[14]. J. A. Tropp, "Algorithms for simultaneous sparse approximation. Part II: Convex relaxation," *Signal Process.*, vol. 86, no. 3, pp. 589–602, 2006

[15]. Y. Li and Y. Chi, "Off-the-grid line spectrum denoising and estimation with multiple measurement vectors," *IEEE Trans. Signal Process*., vol. 64, no. 5, pp. 1257–1269, Mar. 2016.

[16]. S. Subedi, Y. D. Zhang, M. G. Amin, and B. Himed, "Group sparsity based multi-target tracking in passive multistatic radar systems using doppler-only measurements," *IEEE Trans. Signal Process.*, vol. 64, no. 14, pp. 3619–3634, Jul. 2016.

[17]. L. Zelnik-Manor, K. Rosenblum, and Y. C. Eldar, "Sensing matrix optimization for block-sparse decoding," *IEEE Trans. Signal Process.,* vol. 59, no. 9, pp. 4300–4312, Sep. 2011.

[18]. S. Ji, D. Dunson, and L. Carin, "Multitask compressive sensing," *IEEE Trans. Signal Process.,* vol. 57, no. 1, pp. 92–106, Jan. 2009.